Journal Pre-proof

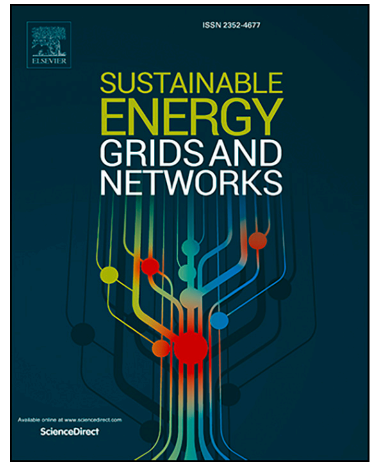


Probabilistic Day-Ahead Battery Scheduling based on Mixed Random Variables for Enhanced Grid Operation

Janik Pinter, Frederik Zahn, Maximilian Beichter, Ralf Mikut, Veit Hagenmeyer

PII: S2352-4677(25)00195-X
DOI: https://doi.org/10.1016/j.segan.2025.101813
Reference: SEGAN 101813

To appear in: *Sustainable Energy, Grids and Networks*

Received Date: 18 November 2024
Revised Date: 26 March 2025
Accepted Date: 23 July 2025

Please cite this article as: Pinter J, Zahn F, Beichter M, Mikut R, Hagenmeyer V, Probabilistic Day-Ahead Battery Scheduling based on Mixed Random Variables for Enhanced Grid Operation, *Sustainable Energy, Grids and Networks* (2025), doi: https://doi.org/10.1016/j.segan.2025.101813.

Bulk Power System Dynamics and Control - XII, June 2025, Sorrento, Italy

# Probabilistic Day-Ahead Battery Scheduling based on Mixed Random Variables for Enhanced Grid Operation

Janik Pinter*, Frederik Zahn*, Maximilian Beichter*, Ralf Mikut*, and Veit Hagenmeyer*
*Institute for Automation and Applied Informatics,*
*Karlsruhe Institute of Technology (KIT), Germany*
*{firstname.lastname}@kit.edu

***Abstract*—The increasing penetration of renewable energy sources introduces significant challenges to the power grid, primarily due to their inherent variability. A new opportunity for grid operation is the smart integration of electricity production combined with battery storages in residential buildings. This study explores how residential battery systems can support the power grid by flexibly managing deviations from forecasted residential power consumption and PV generation. The key contribution of this work is the development of an analytical approach that enables the asymmetric allocation of quantified power uncertainties between a residential battery system and the power grid, introducing a new degree of freedom into the scheduling problem. This is accomplished by employing mixed random variables—characterized by both continuous and discrete events—to model battery and grid power uncertainties. These variables are embedded into a continuous stochastic optimization framework, which computes probabilistic schedules for battery operation and power exchange with the grid. Test cases demonstrate that the proposed framework can be used effectively to quantify and reduce grid uncertainties while maximizing residential self-sufficiency. It is also shown that residential battery systems can be used to actively provide flexibility during critical periods of grid operation. Overall, this framework empowers prosumers to take a more active role in the power grid, contributing to a more resilient and adaptive energy system.**

## I. Introduction

The global transition toward renewable energy generation is transforming electrical power systems worldwide. While renewable energy sources offer significant environmental and economic benefits, they also introduce new challenges due to their intrinsic volatility. Historically, uncertainties in power systems primarily occurred on the demand side and were effectively manageable due to the controllability of conventional power plants, i.e., the generation was able to match the demand. As the penetration of renewable energy sources grows, the controllability on the generation side decreases, leading to a significant increase in overall uncertainties within the power grid. To enable a secure and reliable grid operation in the future, various methods for providing unidirectional flexibility and managing uncertainties at different power and voltage levels are currently being investigated, such as, at

- Grid Level: Large-scale balancing mechanisms and grid-level storage systems are investigated to ensure system-wide stability [1].
- Subgrid Level: Microgrids coordinate local renewable generation, energy storages, and demand-side management to handle uncertainties and reduce dependence on the main grid [2].
- Single Unit: Individual industrial or residential buildings can decrease their power consumption uncertainties by optimized scheduling of energy consumption and Battery Energy Storage System (BESS) operation [3].

The increasing deployment of residential Photovoltaic (PV) systems in conjunction with BESSs demands further investigation on how to best integrate them into power system management. The major sources of uncertainty on a household level are deviations from forecasted consumption profiles and forecasted PV production. BESSs offer great potential to balance these deviations, as opposed to injecting them into the grid. To achieve this, the operation of BESSs needs to take into account the uncertainties in a systematic way. Therefore, the present work focuses on the development of a scheduling approach for a single house. Our approach allows quantification and reduction of grid power injection uncertainties while respecting the physical limits of the BESSs. We present a novel formulation of the stochastic BESS scheduling problem to calculate an optimized day-ahead schedule for residential buildings featuring a PV system.

### A. Related Works

Several studies have proposed methods for optimizing day-ahead BESS scheduling in residential buildings, which differ in two distinct aspects: First, how uncertainties—whether in generation, demand, or electricity prices—are embedded into the optimization process. Second, the specific objective the optimization seeks to achieve.

Uncertainties can be embedded into an optimization framework in multiple ways. One common approach is Robust Optimization (RO), which focuses on optimizing system performance while ensuring feasibility for worst-case realizations. Typically, uncertain parameters are assumed to lie within fixed bounds [4]–[7]. The optimization problem is solved using their worst-case values, i.e., most often the boundary values of the assumed intervals [8]. For example, [4] optimizes the day-ahead scheduling of a smart home equipped with PV and BESS, treating energy prices as uncertain within predefined bounds.

Instead of using worst-case values, uncertainties can also be incorporated into optimization frameworks via scenario-generation techniques [9]–[11]. Methods such as Sample-

Average-Approximations, Markov Chains, and Monte-Carlo approaches create an ensemble of deterministic scenarios, each representing a possible realization of uncertain parameters. These methods transform the stochastic formulation into a more elaborate deterministic one, which allows the use of well-established, computationally efficient optimization techniques. For instance, [9] minimizes residential electricity costs by combining a neural network with an error analysis technique to represent uncertain PV behavior in the form of a scenario ensemble.

However, a critical limitation of uncertainty representation via worst-case values or scenario-generation techniques is their inability to provide quantified uncertainty propagation throughout the optimization process. For our work, the focus is not just on optimal BESS scheduling but also on the power exchange with the grid. Therefore, we require a method that quantifies uncertainties in a coherent and probabilistic manner throughout the optimization process. Neither uncertainty representation via worst-case values nor scenario-generation techniques meet this requirement, which is why we propose a different approach.

In our work, Stochastic Programming (SP) is employed to represent uncertainties in the optimization framework. SP allows for quantified uncertainty propagation by representing uncertain parameters as random variables with known probability distributions. These distributions are typically incorporated into an optimization framework through chance constraints [12]–[14], or by minimizing their expected values [15], [16].

One limitation of SP, however, is that it assumes the probability distributions of random variables are fully known, which does not always reflect reality. This issue is addressed in Distributionally Robust Optimization (DRO) [8]. Instead of relying on a single probability distribution, DRO considers a set of potential probability distributions and optimizes for the worst-case distribution within the set [17]–[19]. However, in our case, the determination of the worst-case distribution is not straightforward because the expected values of the random variables are not fixed but depend on the decision variables, determined during optimization. Thus, while DRO presents an appealing theoretical framework, its practical application is limited for the given case.

In general, cutting costs is the main incentive to optimize BESS operation. This is most commonly achieved by performing peak shaving [20], load shifting [21], price arbitrage operations [15] or maximizing self-sufficiency [22]. Our study investigates the extension of those conventional usages. The fundamental idea, first presented in [3], is that the homeowner communicates its forecasted grid power exchange to the grid operator one day in advance. In the following, this forecasted power exchange is called Dispatch Schedule (DiS). The BESS is used to minimize the deviations from the DiS, without neglecting a residential objective of maximizing self-sufficiency. By doing so, the overall uncertainty in the power grid can be reduced, which leads to a decrease in balancing power requirements and system costs [23]. The framework from [3] is divided into two stages: the day-ahead stage, where the DiS is computed, and the real-time stage, where Model Predictive Control is applied to minimize DiS deviations.

The authors of [12] enhance the proposed framework by incorporating probabilistic power forecasts. They assume that the BESS is able to fully compensate for all deviations from forecasted consumption and PV production profiles. As a result, the DiS remains deterministic, whereas the BESS schedule is probabilistic. To ensure feasibility, the BESS constraints, i.e., its power and capacity limits, are enforced through chance-constraints. These constraints ensure compliance with a given probability, known as security level. This approach focuses on a reliable DiS by shifting all uncertainties toward the residential BESS. However, this limits the ability to minimize electricity costs by exploiting the BESS. Additionally, selecting appropriate security levels and interpreting the individual chance-constraints are challenging themselves [24], and real-world limitations, like BESS response times or ramping constraints, prevent the full compensation of DiS deviations by the BESS on smaller time scales [25].

The authors of [15] investigate a similar probabilistic setting but focus on minimizing residential electricity costs by formulating an exact expectation-based stochastic optimization approach. Convexity of the nonlinear optimization problem is achieved and proven. The uncertainty is handled by assuming that the grid fully compensates for all power uncertainties. Therefore, in contrast to [12], the approach results in a probabilistic DiS and a deterministic BESS schedule. In the latter case, the DiS is more of a by-product instead of a fundamental objective.

To summarize, SP approaches for residential day-ahead BESS scheduling tend to either assign all uncertainties to the grid [15] or to the BESS [12], sidestepping the complexity of allocating uncertainties between the two systems. Approaches, in which BESSs absorb all uncertainties, support the power grid but struggle with interpretability and cost minimization, while methods that shift all uncertainties to the grid optimize costs yet overlook the potential of residential BESSs to provide flexibility. The listed approaches investigate a residential or grid perspective in isolation. However, as the role of prosumers expands, a unified framework that balances both views becomes critical. This gap in integrating both perspectives into a single framework motivates the present work.

### B. Contribution

The main idea of the present work is a formulation of the BESS scheduling problem, which allows to share quantified uncertainties between the grid and the BESS. The challenge lies in effectively representing and managing these uncertainties and incorporating them into a stochastic optimization framework. With that, we aim to lay a foundation that motivates future research to consider grid and prosumer perspectives jointly rather than in isolation. In the present work, we do not schedule set points for the BESS's charging, but we assign intervals of minimum and maximum charging power. This formulation allows to absorb a limited amount of deviations in the BESS while respecting its physical limits and quantifying the uncertainty injected into the grid.

The key contributions of this paper include the following:

1) Formulation of a novel approach to allow an asymmetrical allocation of quantified power uncertainties between a BESS and the power grid using mixed random variables.
2) Derivation of an expectation-based nonlinear stochastic optimization problem to compute probabilistic schedules for BESS operation and grid exchange.
3) Demonstration of the proposed scheduling algorithms for three different scenarios based on real-world data.

The paper is organized as follows: Section II introduces the problem and contains the main contribution of this paper. The core idea on how to tackle uncertainties is presented and a mathematical power exchange model is formulated. In Section III, the derived model is embedded into an optimization framework in a generic form and is applied and analyzed in Section IV. Section V concludes this paper.

## II. Model Derivation

We investigate the combination of a single residential house equipped with PV panels and a BESS. We primarily focus on stationary BESSs but want to mention that the usage of Electric Vehicles (EVs) with bidirectional charging capabilities essentially results in the same model as long as the EVs remain connected to the charging point. For EVs that only allow unidirectional charging, the presented approach would shift more toward demand-side management.

In this study, the inflexible power demand (also referred to as load) is combined with the inflexible PV power generation in the variable $P_L$. It represents both power production and consumption and is therefore referred to as prosumption. The basic structure is sketched in Figure 1. $P_B$ corresponds to the controllable BESS power and $P_G$ denotes the power provided by the grid. In order to fully meet the residential power prosumption and under the assumption of a lossless power connection, the power exchange can be described via

$$P_L = P_B + P_G, \tag{1}$$

with positive power flows defined by the arrows in Figure 1.

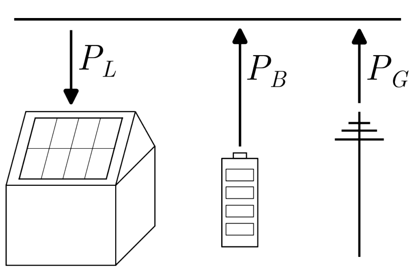


Fig. 1: General setting. Residential prosumption, BESS power, and grid power are in balance: $P_L = P_B + P_G$.

### A. Fundamental Concept

The prosumption $P_L$ of an upcoming time period is inherently uncertain and can only be estimated. In conventional settings, the power grid alone compensates for the difference between estimation and realization. In our approach, we schedule the BESS to have some quantified capacity $\underline{x}$ and $\bar{x}$ reserved during the specific time in question, as depicted in Figure 2. This reserved capacity can be used to reduce the difference between realization and expectation (e.g., $d_{new} = d - \underline{x}$) and thereby ease the burden on the grid. With that, planning reliability increases, and the BESS supports the grid.

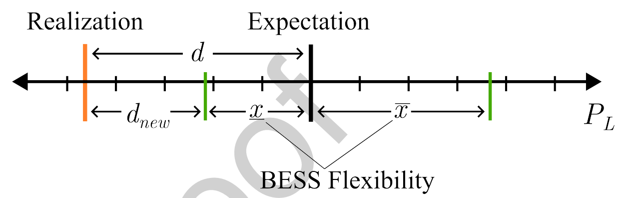


Fig. 2: General principle of the present work. Previously quantified BESS flexibility can be used to decrease the difference $d$ between expected and actual prosumption of a building that needs to be matched by the grid, i.e., in the illustrated example $d_{new} = d - \underline{x}$.

The subsequent chapters essentially explore when, how much, and in which direction BESS flexibility can be provided by adapting $\underline{x}$ and $\bar{x}$, without significantly affecting expected residential self-sufficiency. They also investigate how a grid operator can take advantage of the insights gained by the flexibility offered to enable a better understanding of upcoming grid conditions.

### B. Uncertainty Modeling

In this work, the prosumption is modeled as a real-valued random variable $P_L\colon \Omega \to \mathbb{R}$ defined on a probability space $(\Omega, \mathcal{F}, \mathbb{P})$, where $\Omega$ is the set of possible outcomes, $\mathcal{F}$ is a sigma-algebra of measurable events, and $\mathbb{P}$ is a probability measure. $P_L$ represents the average power exchange over a specific time period[1] and is assumed to be absolutely continuous, implying that a Probability Density Function (PDF) $f_{P_L}$ exists.

We split the prosumption

$$P_L = \hat{p}_L + \Delta P_L \tag{2}$$

into $\hat{p}_L = \mathbb{E}[P_L]$, where $\mathbb{E}[\cdot]$ refers to the expected value, and $\Delta P_L$, which denotes the deviations from the expected value. Consequently, $\mathbb{E}[\Delta P_L] = 0$ holds by definition. The same formulation can be found in [12] or [15]. The PDF $f_{P_L}$ is not assumed to follow any specific distribution (e.g., Gaussian) but needs to be available in a parametric form so that its integral over a specific domain can be computed. With that, the PDF referring to the deviations from the expected value can be expressed as $f_{\Delta P_L}(z) = f_{P_L}(z + \hat{p}_L)$.

[1]For the sake of simplicity, the time index is omitted in this subsection.

### C. Uncertainty Allocation

The main idea of the present work is the partitioning of the uncertain prosumption deviation $\Delta P_L$ into two parts, i.e., one part that is fed into the BESS, and one part that is injected into the grid. To this end, we introduce an upper and a lower bound of BESS charging power, i.e., $\underline{x} \in \mathbb{R}_0^-$ and $\bar{x} \in \mathbb{R}_0^+$. The prosumption uncertainty in the interval $[\underline{x}, \bar{x}]$ is assigned to the BESS, and the remaining uncertainty is injected into the grid. We introduce two random variables that depend on $\Delta P_L$, i.e.,

$$\Delta P_{L\to B} = \begin{cases} \underline{x} & \Delta P_L \leq \underline{x} \\ \Delta P_L & \underline{x} < \Delta P_L < \bar{x} \\ \bar{x} & \bar{x} \leq \Delta P_L \end{cases} \tag{3a}$$

$$\Delta P_{L\to G} = \begin{cases} \Delta P_L - \underline{x} & \Delta P_L \leq \underline{x} \\ 0 & \underline{x} < \Delta P_L < \bar{x} \\ \Delta P_L - \bar{x} & \bar{x} \leq \Delta P_L. \end{cases} \tag{3b}$$

$\Delta P_{L\to B}$ and $\Delta P_{L\to G}$ represent the prosumption uncertainties that are shifted to the BESS or the grid, respectively. With that, $\underline{x}$ and $\bar{x}$ reflect the minimal and maximal deviation from the expected prosumption $\hat{p}_L$ that is still fully compensated by the BESS. Note that $\underline{x}$ and $\bar{x}$ do not result from any forecasting process but can be chosen freely[2] and thus be integrated into an optimization framework as decision variables, see Section III. For more information on the general transformation of random variables, see [26] or [27]. Additionally, it should be noted that

$$\Delta P_{L\to B} + \Delta P_{L\to G} = \Delta P_L \tag{4}$$

holds by definition. This simply means that the sum of $\Delta P_{L\to B}$ and $\Delta P_{L\to G}$ accounts for the total prosumption uncertainty $\Delta P_L$.

Figure 3a illustrates an exemplary uncertainty allocation, with all uncertainty realizations within the interval $[\underline{x}, \bar{x}]$ being fully compensated by the BESS alone. This choice of compensation is advantageous since prosumption PDFs typically have larger values around their expected values than in areas further away, essentially reducing the probability of compensation by the grid. For realizations outside of $[\underline{x}, \bar{x}]$, the occurring power discrepancy is provided by the BESS and the grid combined as sketched in Figure 2.

Furthermore, it should be noted that $\Delta P_{L\to B}$ and $\Delta P_{L\to G}$ contain both continuous and discrete parts, classifying them as so-called mixed random variables [26]. The handling and interpretation of mixed random variables are not always apparent [28], but they have been proven useful to model different phenomena with mostly zero-inflated data such as air contamination [29] or rainfall events [30]. However, what sets our work apart from most research on mixed random variables is that the mixed distribution is intentionally designed, whereas in related studies, mixed distributions typically arise as natural phenomena from data. Rather than addressing the challenges posed by mixed distributions, this paper emphasizes the advantageous properties of mixed random variables and explores how they can be leveraged for modeling BESS scheduling.

### D. Computation of Mixed Distribution Functions and Expected Values

For a continuous random variable $X$ with PDF $f_X$, the resulting distribution $f_Y$ of a mixed transformation $Y = g(X)$ can be derived by the superposition of continuous parts $f_{Y_C}$ and discrete parts $f_{Y_D}$ according to $f_Y(y) = f_{Y_C}(y) + f_{Y_D}(y)$. The two terms are derived and explained in [26] and can be computed according to

$$f_{Y_C}(y) = \sum_{i=1}^{N} \frac{f_X(x)}{\left|\frac{dy}{dx}\right|}\Bigg|_{x_i = g_i^{-1}(y)} \tag{5a}$$

$$f_{Y_D}(y) = \sum_{i=1}^{M} \mathbb{P}(Y = y_{D,i})\delta(y - y_{D,i}). \tag{5b}$$

$N$ denotes the number of continuous parts of the mixed transformation, whereas $M$ refers to the number of discrete parts. In Equation (5a), it is assumed that the inverses of the continuous parts of the transformation $g_i^{-1}$ exist.[3] $y_{D,i}$ are discrete events, and $\delta$ is the Dirac delta function. With that the PDFs[4] of $\Delta P_{L\to B}$ and $\Delta P_{L\to G}$ can be computed using the unit step function $U(z)$:

$$\begin{aligned} f_{\Delta P_{L\to B}}(z) = {} & p_1\delta(z - \underline{x}) + p_2\delta(z - \bar{x}) \\ & + f_{\Delta P_L}(z)[U(z - \underline{x}) - U(z - \bar{x})] \end{aligned} \tag{6a}$$

$$\begin{aligned} f_{\Delta P_{L\to G}}(z) = {} & (1 - p_1 - p_2)\delta(z) + f_{\Delta P_L}(z + \bar{x})U(z) \\ & + f_{\Delta P_L}(z + \underline{x})[1 - U(z)], \end{aligned} \tag{6b}$$

where the probabilities $p_1 = \mathbb{P}(\Delta P_L < \underline{x}) = \mathbb{P}(\Delta P_{L\to B} = \underline{x}) = \mathbb{P}(\Delta P_{L\to G} < 0)$ and analogously $p_2 = \mathbb{P}(\Delta P_{L\to B} = \bar{x})$ correspond to the discrete events. The unit step function $U(z)$ restricts the domains in which the continuous parts are defined. The resulting PDF of the BESS power uncertainty is illustrated in Figure 3b. The uncertainties of the original prosumption outside the interval $[\underline{x}, \bar{x}]$ are mapped to the discrete events $\underline{x}$ or $\bar{x}$ respectively, effectively limiting the maximal and minimal BESS power deviation to a fixed interval. The other portion of the prosumption uncertainty remains unchanged. Figure 3c displays the uncertainties shifted to the grid as a zero-inflated distribution; all uncertainties within $[\underline{x}, \bar{x}]$ are mapped to zero, whereas the uncertainty tails are shifted

[2] To be precise, $\underline{x}$ and $\bar{x}$ can be chosen freely, but they are constrained, i.e., they are restricted by $\underline{x} \leq 0$, $\bar{x} \geq 0$, and the respective BESS's physical limits defined in Section II-E.

[3] In our case, the inverse functions are $g_1^{-1}(\Delta P_{L\to B}) = \Delta P_{L\to B}$ for the BESS, and $g_1^{-1}(\Delta P_{L\to G}) = \Delta P_{L\to G} + \underline{x}$ and $g_2^{-1}(\Delta P_{L\to G}) = \Delta P_{L\to G} + \bar{x}$ for the grid.

[4] When dealing with mixed random variables, the term *probability density function* is sometimes used to describe the entire distribution, even though this is not mathematically precise. A PDF applies to continuous components only, while a Probability Mass Function (PMF) refers to discrete ones. Since no standard term covers both aspects of mixed distributions, the term PDF is used in the present paper for simplicity.

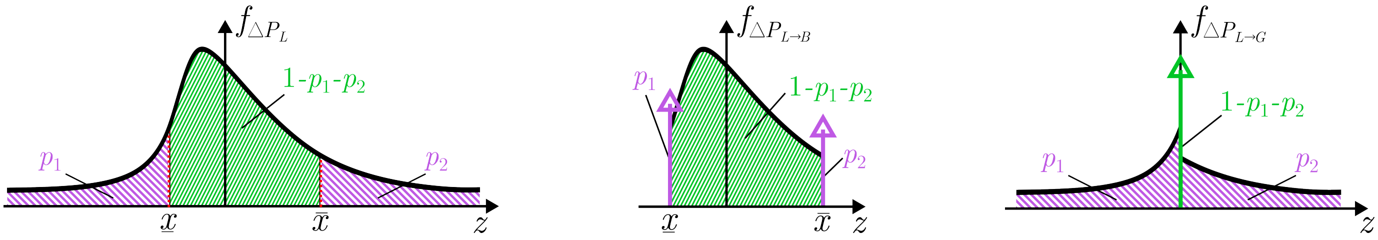

(a) Prosumption PDF (b) BESS Power PDF (c) Grid Power PDF

Fig. 3: The continuous prosumption PDF (a) can be represented by the two dependent distributions (b) and (c), containing continuous and discrete parts. The BESS power uncertainty (b) is defined over a closed interval. The grid power uncertainty (c) contains a discrete event at zero.

horizontally but remain otherwise untouched. It can easily be seen that all displayed distributions are valid as they are all non-negative and integrate to one (see Figure 3).

Furthermore, due to the independent choice of $\underline{x}$ and $\bar{x}$, the uncertainties can be asymmetrically allocated between the grid and the BESS. This property is shown to be useful in Section IV, but also implies that the deviations $\Delta P_{L\to B}$ and $\Delta P_{L\to G}$ can have non-zero expected values, i.e.,

$$\mathbb{E}[\Delta P_{L\to B}] = p_1 \underline{x} + \int_{\underline{x}}^{\bar{x}} z f_{\Delta P_L}(z)\, dz + p_2 \bar{x} \tag{7a}$$

$$\begin{aligned} \mathbb{E}[\Delta P_{L\to G}] = &\int_{-\infty}^{0} z f_{\Delta P_L}(z+\underline{x})\, dz \\ &+ \int_{0}^{\infty} z f_{\Delta P_L}(z+\bar{x})\, dz. \end{aligned} \tag{7b}$$

Because the expected value of a sum of random variables is equal to the sum of their individual expected values, regardless of whether they are independent [26],

$$\begin{aligned} \mathbb{E}[\Delta P_L] &= \mathbb{E}[\Delta P_{L\to B} + \Delta P_{L\to G}] \\ &= \mathbb{E}[\Delta P_{L\to B}] + \mathbb{E}[\Delta P_{L\to G}] = 0 \end{aligned} \tag{8}$$

is valid and can be either used as an alternative to Equation (7a) or Equation (7b), or simply for validation purposes.

### *E. Battery State Evolution*

In this section, the BESS model with its state evolution is derived. We describe the state evolution in discrete time with time variable $k \in \mathcal{K} \subset \mathbb{N}_0$. Because of the described probabilistic approach with the allocation of uncertainties in Section II-C, the BESS energy state becomes a random variable $E$, which we split into two parts, i.e.,

$$E(k) = e(k) + \Delta E(k). \tag{9}$$

$e(k) \in \mathbb{R}$ is introduced as the nominal battery state and reflects the energy state based on the previous expected prosumptions $\hat{p}_L$, whereas the probabilistic battery state $\Delta E(k)$ is a random variable that represents the deviations from the nominal battery state. With that, $\Delta E(k)$ depends on the previous probabilistic prosumptions $\Delta P_L$. To be concise,

$$\begin{aligned} e(k) &= h_1(\hat{p}_L(k), \hat{p}_L(k-1), ..., \hat{p}_L(0)) \\ \Delta E(k) &= h_2(\Delta P_L(k), \Delta P_L(k-1), ..., \Delta P_L(0)), \end{aligned}$$

with $e(k)$ explicitly not depending on $\Delta P_L$ and $\Delta E(k)$ not depending on $\hat{p}_L$.[5] It is important to note that even though the nominal battery state $e$ corresponds to the expected prosumption, it does not reflect the expected battery state, hence the different name. This phenomenon arises due to the handling of asymmetric prosumption PDFs as well as the possibility of asymmetric uncertainty shifts. The nominal battery state $e$ coincides with the expected battery state $\mathbb{E}[E]$ only if Equation (7a) permanently equals zero. This behavior is exemplarily analyzed in Section IV-B.

The BESS power can be described with a similar approach via

$$P_B(k) = p_B(k) + \Delta P_{L\to B}(k) \tag{10}$$

with $p_B$ being the nominal battery power.

The evolution of the BESS state can be formulated:

$$\begin{aligned} E(k+1) &= E(k) - tP_B(k) - t\mu \left|P_B(k)\right| \\ &= e(k) + \Delta E(k) - tp_B(k) - t\Delta P_{L\to B}(k) \\ &\quad - t\mu \left|p_B(k) + \Delta P_{L\to B}(k)\right|. \end{aligned} \tag{11}$$

The variable $\mu$ is a loss coefficient that models charging and discharging losses, $t$ denotes the time between the discrete time points $k$ and $k+1$. To separate evolution of the nominal and probabilistic battery states, $E$ is approximated by using the triangle inequality $|a+b| \leq |a| + |b|$:

$$\begin{aligned} E(k+1) &= e(k) + \Delta E(k) - tp_B(k) - t\Delta P_{L\to B}(k) \\ &\quad - t\mu \left|p_B(k) + \Delta P_{L\to B}(k)\right| \\ &\geq e(k) + \Delta E(k) - tp_B(k) - t\Delta P_{L\to B}(k) \\ &\quad - t\mu \left|p_B(k)\right| - t\mu \left|\Delta P_{L\to B}(k)\right|. \end{aligned} \tag{12}$$

This is justifiable because only comparatively small portions of the total energy state are approximated, i.e., the BESS's

[5] To be precise, $\Delta E(k)$ depends on $\Delta P_{L\to B}(k)$, which according to Equation 3a, depends on $\Delta P_L(k)$. Similarly, $e(k)$ depends on $p_B(k)$ which depends on $\hat{p}_L(k)$, as derived later in Subsection II-F.

losses. Additionally, this approximation can be considered conservative since the total energy state is underestimated.

Hence, the nominal battery state evolution

$$e(k+1) = e(k) - tp_B(k) - t\mu\,|p_B(k)| \qquad (13)$$

and the probabilistic evolution

$$\Delta E(k+1) = \Delta E(k) - t\Delta P_{L\to B}(k) - t\mu\,|\Delta P_{L\to B}(k)| \qquad (14)$$

can be formulated separately. Equation (14) consists of the sum of three random variables, making its computation challenging. If one neglects stochastic losses $\mu\,|\Delta P_{L\to B}(k)| \approx 0$ and assumes independence of prosumption between subsequent time increments $\Delta P_L(k)$ and $\Delta P_L(k+1)$ $\forall k \in \mathcal{K}$, the probabilistic battery state can be computed by convolution. However, such an assumption is difficult to justify: For instance, even a simple unforeseen cloud formation can affect a PV's power production over several time increments, an effect that would be entirely overlooked under this assumption. Consequently, some BESS operation models are specifically designed to account for this dependence through sequential decision-making processes [31], [32]. An alternative method to compute Equation (14) would involve finding a suitable approximation of the joint probability function. In [33], a way to approximate a joint dependence for probabilistic load forecasting using empirical copulas is presented. However, applying such an approach to the problem at hand is challenging due to the complex dependence between probabilistic battery power and probabilistic battery state, where the latter essentially encapsulates all prior uncertainties of probabilistic battery power. This complexity is further compounded by the fact that the probabilistic battery state is influenced by decision variables $\underline{x}(k)$ and $\bar{x}(k)$, which are supposed to be found by solving a subsequent optimization problem.

Although a suitable solution for solving Equation (14) has not yet been identified, the equation remains valuable for our approach: The restriction of BESS power uncertainties to the fixed interval $[\underline{x}(k), \bar{x}(k)]$ (see Figure 3b) implies that the resulting energy uncertainty accumulated in the BESS is also bounded. This insight can be used to calculate the evolution of the minimum and maximum battery state based on Equation (14):

$$\Delta E_{\min}(k+1) = \Delta E_{\min}(k) - t\bar{x}(k) - t\mu\bar{x}(k) \qquad (15a)$$

$$\Delta E_{\max}(k+1) = \Delta E_{\max}(k) - t\underline{x}(k) + t\mu\underline{x}(k), \qquad (15b)$$

with $\underline{x}(k) \leq 0$ and $\bar{x}(k) \geq 0$. Therefore, we can compute the minimum and maximum battery states, the nominal battery state, and the expected battery state (which can be derived from Equation (7a)). Nevertheless, the lack of a full distribution function of the BESS state is a limitation of the model depicted. This restricts the ability to shift BESS uncertainties to the grid, meaning the uncertainty bandwidth within the BESS is non-decreasing.

Typically, the BESS energy and power constraints are expressed as

$$E(k) \overset{!}{\in} [\underline{e}, \bar{e}] \qquad (16a)$$

$$P_B(k) \overset{!}{\in} [\underline{p}_B, \bar{p}_B], \qquad (16b)$$

with $\underline{e}$, $\bar{e}$ and $\underline{p}_B$, $\bar{p}_B$ being the minimum and maximum BESS capacity and power, respectively. In our approach, the BESS constraints can be reformulated to

$$e(k) + \Delta E_{\min}(k) \geq \underline{e} \qquad (17a)$$

$$e(k) + \Delta E_{\max}(k) \leq \bar{e} \qquad (17b)$$

$$p_B(k) + \underline{x}(k) \geq \underline{p}_B \qquad (17c)$$

$$p_B(k) + \bar{x}(k) \leq \bar{p}_B. \qquad (17d)$$

Their compliance can be ensured at all times, implying that the physical constraints of the BESS are respected.

### F. Grid Exchange

The grid power

$$P_G = p_G + \Delta P_{L\to G} \qquad (18)$$

is divided into two components - nominal and probabilistic - mirroring the partitioning of the BESS power in Equation (10). Based on the lossless power connection in Equation (1), the prosumption uncertainty allocation in Equation (4) and the partitioning of random variables in two parts in Equation (2), (10) and (18), it directly follows that

$$\hat{p}_L = p_B + p_G. \qquad (19)$$

It can be seen that even though the nominal powers $p_B$ and $p_G$ both depend on the expected prosumption $\hat{p}_L$, they do not reflect the respective expected power. This discrepancy arises because the additional expected values of $\Delta P_{L\to B}$ and $\Delta P_{L\to G}$ (see Equation (7a) and (7b)) cancel each other out during the derivation.

In the following, $p_G$ represents the deterministic Dispatch Schedule (DiS), while $\Delta P_{L\to G}$ describes the deviations from the DiS probabilistically. These deviations should be minimized, ideally being zero. With the chosen structure of $\Delta P_{L\to G}$ to specifically include zero-inflated events, deviations of zero can appear with non-zero probability (see Figure 3c).

## III. Optimization Problem

This chapter presents the derived model within an optimization framework. The framework maps probabilistic inputs to fully probabilistic outputs in order to enable comprehensive uncertainty quantification. As outlined in Section II-A, the framework also provides insights into when, to what extent, and in which direction BESS flexibility can be offered (i.e., to find optimized values for $\underline{x}(k)$ and $\bar{x}(k)$) without neglecting the incentive of maximizing residential self-sufficiency. The optimization problem is formulated as follows:

$$\min_{p_B,\underline{x},\bar{x}} C(p_G^+,\ p_G^-,\ p_B^+,\ p_B^-,\ p_1,\ p_2,\ \mathbb{E}[\Delta P_{L\to G}^{<0}],\ \mathbb{E}[\Delta P_{L\to G}^{>0}])$$

s.t. for all $k \in \mathcal{K}$

$$e(k+1) = e(k) - tp_B(k) - t\mu p_B^+(k) + t\mu p_B^-(k) \tag{20a}$$

$$\Delta E_{\min}(k+1) = \Delta E_{\min}(k) - t\bar{x}(k) - t\mu\bar{x}(k) \tag{20b}$$

$$\Delta E_{\max}(k+1) = \Delta E_{\max}(k) - t\underline{x}(k) + t\mu\underline{x}(k) \tag{20c}$$

$$e(k) + \Delta E_{\min}(k) \geq \underline{e} \tag{20d}$$

$$e(k) + \Delta E_{\max}(k) \leq \bar{e} \tag{20e}$$

$$p_B(k) + t\underline{x}(k) \geq \underline{p}_B \tag{20f}$$

$$p_B(k) + t\bar{x}(k) \leq \bar{p}_B \tag{20g}$$

$$p_G(k) = \hat{p}_L(k) - p_B(k) \tag{20h}$$

$$\mathbb{E}[\Delta P_{L\to G}^{<0}(k)] = \int_{-\infty}^{0} z f_{k,\Delta P_L}(z + \underline{x}(k))\, dz \tag{20i}$$

$$\mathbb{E}[\Delta P_{L\to G}^{>0}(k)] = \int_{0}^{\infty} z f_{k,\Delta P_L}(z + \bar{x}(k))\, dz \tag{20j}$$

$$p_1(k) = \int_{-\infty}^{\underline{x}(k)} f_{k,\Delta P_L}(z)\, dz \tag{20k}$$

$$p_2(k) = 1 - \int_{-\infty}^{\bar{x}(k)} f_{k,\Delta P_L}(z)\, dz \tag{20l}$$

$$p_G(k) = p_G^+(k) + p_G^-(k) \tag{20m}$$

$$-p_G^+(k) \cdot p_G^-(k) \leq 10^{-8} \tag{20n}$$

$$p_G^+(k) \geq 0, \quad p_G^-(k) \leq 0 \tag{20o}$$

$$p_B(k) = p_B^+(k) + p_B^-(k) \tag{20p}$$

$$-p_B^+(k) \cdot p_B^-(k) \leq 10^{-8} \tag{20q}$$

$$p_B^+(k) \geq 0, \quad p_B^-(k) \leq 0 \tag{20r}$$

$$\underline{x}(k) \leq 0 \tag{20s}$$

$$\bar{x}(k) \geq 0. \tag{20t}$$

The decision variables of the problem are $p_B(k)$, $\underline{x}(k)$ and $\bar{x}(k)$. The input variables, i.e., $\hat{p}_L(k)$ and $f_{k,\Delta P_L}(z)$, are the result of a preceding probabilistic forecasting process.

Equations (20a-20c) refer to the BESS state evolutions. Instead of having fixed scheduling set points, the charging power and the energy state are characterized by respective bounds. Equations (20d-20g) ensure compliance with the BESS's physical limits. Equation (20h) computes the nominal grid power $p_G$, which is used as the basis for the DiS. Thus, deviations from $p_G$ must be quantified, which is described in Equations (20i-20l). To elaborate, incorporating $p_1$ and $p_2$ into the cost function minimizes the likelihood of deviations from the computed DiS. Specifically, $p_2$ accounts for the probability of requiring more power, while $p_1$ addresses the probability of needing less, as visualized in Figure 3. Additionally, the extent of these deviations can be captured through $\mathbb{E}[\Delta P_{L\to G}^{<0}]$ and $\mathbb{E}[\Delta P_{L\to G}^{>0}]$, which represent the expected magnitude of downward or upward deviations, as defined by Equation (7b). The respective integrals depend on the decision variables and thus need to be computed dynamically during the optimization process. For that, the integrals are approximated using numerical integration, specifically, Simpson's 1/3 rule [34].

The nominal grid power $p_G$ is split into two mutually exclusive components in Equations (20m-20o): a positive $p_G^+$ and a negative $p_G^-$. This enables the cost function to define electricity purchase and sale prices separately, making it possible to model more realistic market scenarios. The nominal battery power $p_B$ is divided similarly to accurately account for energy losses.

To summarize, the presented method is an expectation-based nonlinear stochastic optimization problem that is suitable for typical BESS applications, such as maximizing self-sufficiency, as well as actively reducing quantified grid uncertainties. Thereby, the key innovation lies in the analytical and coherent treatment of uncertainties described by mixed random variables. Unlike previous approaches, where uncertainties are either entirely absorbed by the grid [15] or fully shifted into the BESS [12], the presented method enables a quantified and somewhat balanced distribution of uncertainties between the BESS and the grid. This allows the optimization problem to simultaneously compute an optimized probabilistic grid and probabilistic BESS schedule—a capability that, to the best of the authors' knowledge, has not yet been published and analyzed in the literature. This versatility opens up a wide range of potential applications, several of which are analyzed in the following section.

## IV. Model Application

This section presents the application of the proposed model, highlighting different features in three distinct cases. Based on real-world data, we compute probabilistic prosumption forecasts and solve a day-ahead optimization problem for three different cost functions. In Case 1, the model aims to maximize the household's self-sufficiency. Case 2 extends Case 1 by additionally minimizing prosumption uncertainties within the grid. Case 3 combines maximizing self-sufficiency with minimizing grid uncertainties during a critical time period.

The model is implemented in Python using the optimization modeling language Pyomo [35] with IPOPT [36] as the solver.[6] All optimization processes are solved on a laptop with an Intel Core i7-1355U CPU at 1.70 GHz and 32 GB RAM in less than one minute.

### A. Experimental Setup

We use the openly available power data from the Open Power System Data platform [38] of a single residential house referenced in the dataset as 'residential4' located in

[6] The implementation is published as an open-access repository along with this paper [37]. All presented results can be reproduced using the provided code.

southern Germany. This specific building is characterized by a high PV output that exceeds its consumption most of the time. Therefore, the net prosumption is mostly negative. The available data covers the years 2016 to 2018 and serves as the basis for creating the probabilistic forecasts.

To obtain forecasts, we use the neural network time series forecasting library NeuralForecast from Nixtla [39] and employ AutoPatchTST. AutoPatchTST is a hyperparameter optimization using the Patch Time Series Transformer (PatchTST) model from [40]. In our case, we use PatchTST to predict residential prosumption for a 24-hour horizon with an hourly resolution starting at 06:00. The model is trained in an autoregressive manner, relying on historical prosumption data, see [37] for further implementation details. For model training, the first 365 days of data are used as the training set, while the subsequent 200 days are reserved for validation. We evaluate 2500 randomly chosen hyperparameter configurations and select the best-performing model based on its performance on the validation set. The forecast model outputs 99 predicted quantiles that represent the 1% to 99% quantiles in 1% increments. To refine the forecasted outputs, the 99 predicted quantiles are sorted and smoothed using a post-processing approach, see [37].

In order to incorporate the forecasts into the optimization framework, they must be available in parametric form. In the present study, the uncertainties are represented by random variables whose PDFs are assumed to follow the sum of two normal distributions:

$$f_{P_L}(z) = \frac{1}{\sqrt{2\pi}}\left(\frac{\omega_1}{\sigma_1} e^{\frac{-(z-\mu_1)^2}{2\sigma_1^2}} + \frac{\omega_2}{\sigma_2} e^{-\frac{(z-\mu_2)^2}{2\sigma_2^2}}\right). \tag{21}$$

The weights $w_i, \mu_i, \sigma_i, i \in [1,2]$ are obtained via a fitting process to the 99 forecasted quantiles for each hour of each day separately. This form is selected for its ability to capture the asymmetry often observed in real prosumption data. Figure 4 illustrates the forecasted prosumption for a typical day of the selected building. The respective PDFs vary over time in their level of asymmetry, shape, and total variance, see Figure 5.

The cost function of the optimization problem is chosen so that the total power exchange with the grid $p_G^2$ and the impact and probability of deviations from the DiS can be minimized, i.e.,

$$\begin{aligned} C = \sum_{k=0}^{K} & c_1 {p_{G,k}^{+}}^2 + c_2 {p_{G,k}^{-}}^2 + c_3 p_{1,k} \mathbb{E}[\Delta P_{L\to G,k}^{>0}] \\ & - c_4 p_{2,k} \mathbb{E}[\Delta P_{L\to G,k}^{<0}]. \end{aligned} \tag{22}$$

The probabilistic forecasts are fed into three optimization problems, distinguished by the cost-function weights specified in Table I. In general, by choosing the ratio $c_1/c_2$, the user can specify whether positive and negative grid exchange is penalized differently, as is commonly the case due to differences between the costs of purchasing electricity and revenues earned from selling it. The relation $c_3/c_4$ allows to model scenarios where upward and downward deviations from the DiS are penalized differently. Finally, the relationship between

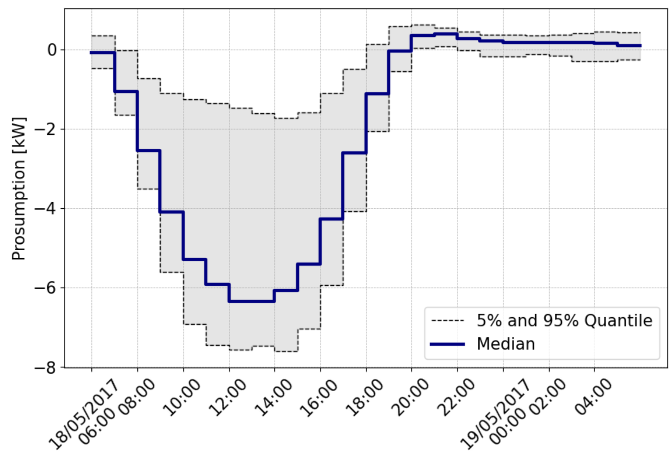


Fig. 4: Forecasted residential prosumption $P_L$ for a typical day. The PV production is expected to dominate the consumption most of the time.

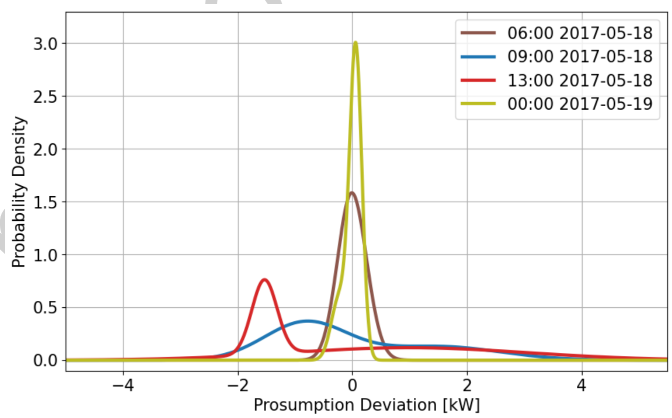


Fig. 5: The overall shape, variance, and level of asymmetry of the forecasted prosumption PDFs $f_{\Delta P_L}$ vary highly throughout the day. All PDFs have an expected value of zero.

$c_1, c_2$ and $c_3, c_4$ highly depends on the specific goal the user wants to achieve, which is why we investigate three distinct cases.

In Case 1, the only objective is to find a DiS that maximizes residential self-sufficiency. The weights $c_3$ and $c_4$ are set to zero, indicating that deviations from the DiS are not penalized. With that, this case reflects the currently dominating market scenario where no financial incentive for uncertainty management for individual buildings is given. As a result, the optimization neither penalizes grid uncertainties nor uncertainties inside the BESS. Consequently, $\underline{x}$ and $\bar{x}$ are dispensable decision variables and are therefore set to zero. This formulation leads to a deterministic BESS schedule, with all uncertainties shifted toward the grid. For Case 2, the primary objective remains to find a DiS that maximizes self-sufficiency. Additionally, deviations from the DiS are slightly penalized. Lastly, Case 3 seeks to balance maximizing self-sufficiency with reducing downward grid deviations during a critical time period. This case reflects a foreseeable future event in which high downward DiS deviations would be unfavorable. For example, suppose a power line is expected to operate near full capacity and is at risk of overheating due to expected high PV generation peaks [41], it may make sense to plan to use a BESS to partially compensate for even higher potential PV generation peaks, thereby reducing the impact of critical situations as well as the likelihood of their occurrence. For all three cases, standard BESS parameters [42] are used, see Table II.

TABLE I: Selected cost-function weights.

| Test Case | $c_1$ | $c_2$ | $c_3$ | $c_4$ |
|---|---|---|---|---|
| **Case 1** | 2 | 1 | 0 | 0 |
| **Case 2** | 2 | 1 | 0.5 | 0.5 |
| **Case 3** | 2 | 1 | 0.5 | 50 for $k \in$ [12:00 - 14:00], 0.5 otherwise |

## B. Results

The results of the three introduced cases are presented in Figure 6, Figure 7, and Figure 8. The figures on the left-hand side display the BESS schedules, while the figures on the right-hand side illustrate the corresponding probabilistic DiSs. The BESS schedules are characterized by four different BESS states, as introduced in Section II-E.

The probabilistic DiSs provide the nominal grid trajectory, see Section II-F. In addition, the probabilities of deviations from the nominal grid power are color encoded, with downward and upward deviations shown separately. To capture the plausible range of these deviations, the 5% and 95% quantiles are displayed as well. Moreover, the conditional expectations of downward and upward deviations are included, indicating the magnitude of expected deviations at any given time if deviations occur. Overall, the variance in prosumption is significantly higher during the day compared to nighttime, reflected in broader probabilistic DiSs during the day across all three cases. The impact of the different battery scheduling approaches on the centered 50%-prediction interval of the grid power are visualized in Figures 9 and 10.

In the following, the results for the three cases are analyzed separately.

*1) Case 1:* The objective is to find a DiS that maximizes residential self-sufficiency. Since the BESS is not used to compensate for uncertainties, the minimum and maximum battery states coincide, resulting in a deterministic BESS schedule. This behavior mirrors the underlying framework of [15], where all uncertainties are expected to be compensated by the grid.

As a result, the probabilities of upward and downward grid deviations always sum up to one, e.g., from 07:00 to 18:00 the probabilities of upward deviations hover around 40% and the probabilities of downward deviations consequently stay around 60%, as indicated by the shading. This asymmetric behavior results directly from the asymmetric nature of the forecasts shown in Figure 4.

At the start of the schedule, the BESS is discharged because, for midday, dominating PV generation is expected. This is incentivized by the quadratic dependence of the nominal grid power $p_G^2$ in the objective, which helps to prevent discharging peaks later in the day. This strategy allows the BESS to fully utilize its capacity to accommodate the expected high PV generation, leading to a plateau in the nominal grid power, see Figure 6b.

In this study, BESS degradation processes are neglected for simplicity, leading to an optimal strategy of fully discharging and then fully charging the BESS. To obtain a more accurate solution, BESS degradation can be directly embedded into the objective function. For example, this could be achieved by integrating the expected BESS power into a BESS degradation model, as investigated in [15] for a deterministic BESS schedule.

*2) Case 2:* The primary objective remains to find a DiS that maximizes self-sufficiency. However, the non-zero weights $c_3$ and $c_4$ reflect that a secondary objective is to minimize grid uncertainties.

The primary objective translates to first discharging and then fully charging the BESS, or more precisely, operating the nominal battery state from 0% to 100% capacity. For the nominal battery state to reach 0% (or 100%) capacity, no upward (or downward) grid uncertainties can be shifted toward the BESS. Only after the corresponding BESS limit has been reached, the BESS can be used for the secondary objective, i.e., to reduce grid uncertainties. In this case, after the nominal battery state leaves 0% capacity at 09:00, the BESS is used to compensate for upward grid uncertainties, i.e., the green area beneath the nominal battery state in Figure 7c. After leaving 100% capacity at 20:00, the BESS is used to compensate for downward grid uncertainties, i.e., the green area above the nominal battery state.

As a result, mostly upward grid uncertainties are compensated by the BESS, i.e., the probabilities of upward grid deviations stay around 25%, whereas the probabilities of downward grid deviations remain around 60%. This asymmetric compensation arises from the truncation of PDFs according to Figure 3b. The maximum battery state aligns with the nominal battery state for the hours 06:00 to 20:00, which indicates that $\underline{x} = 0$ during that timeframe. Consequently, because the distance between the minimum battery state and the nominal battery state grows over time starting at 09:00, $\bar{x} \neq 0$ holds. With that, it follows that the expectation of battery power uncertainty $\mathbb{E}[\Delta P_{L \to B}] \neq 0$ (see Equation (7a)) and, therefore, the expected battery state differs from the nominal battery state. To summarize, the asymmetric uncertainty compensation ($\underline{x} = 0, \bar{x} \neq 0$) results in the difference between the nominal and expected battery state.

TABLE II: Selected BESS specifications.

| $\underline{e}$ [kWh] | $\bar{e}$ [kWh] | $\underline{p}_B$ [kW] | $\bar{p}_B$ [kW] | $\mu$ [%] |
|---|---|---|---|---|
| 0.0 | 13.5 | -5.0 | 5.0 | 5.0 |

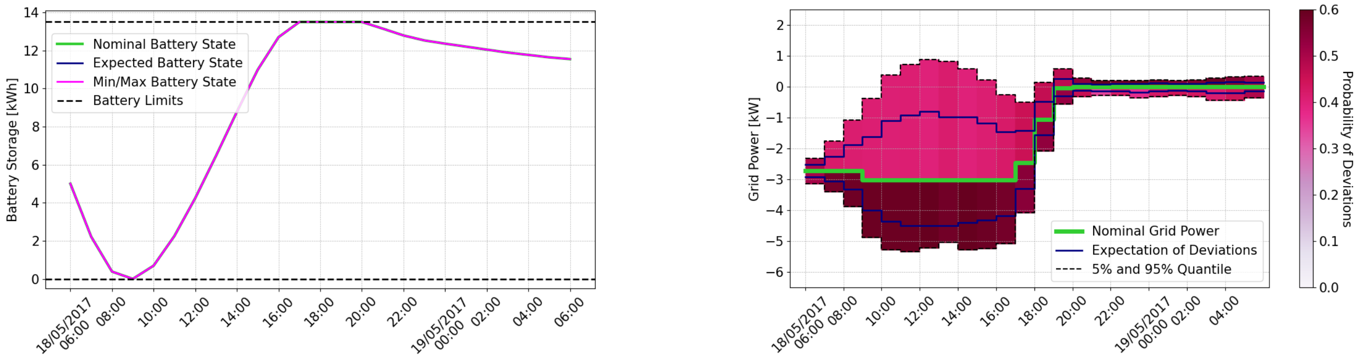


(a) Deterministic BESS Schedule (b) Probabilistic Dispatch Schedule

Fig. 6: Case 1 - Maximizing residential self-sufficiency. All BESS states coincide, making the BESS schedule deterministic. All uncertainties are shifted toward the grid.

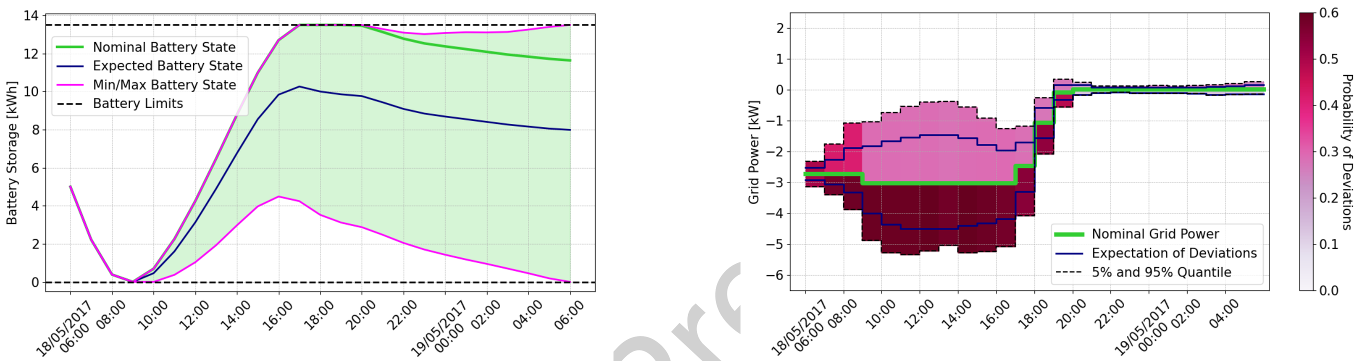


(c) Probabilistic BESS Schedule (d) Probabilistic Dispatch Schedule

Fig. 7: Case 2 - Maximizing residential self-sufficiency while relieving the grid. The BESS reduces grid uncertainties without jeopardizing its main objective of enhancing self-sufficiency. Note that the nominal grid power of Case 1 and Case 2 align, indicating that both cases commit to a schedule with the same level of self-sufficiency.

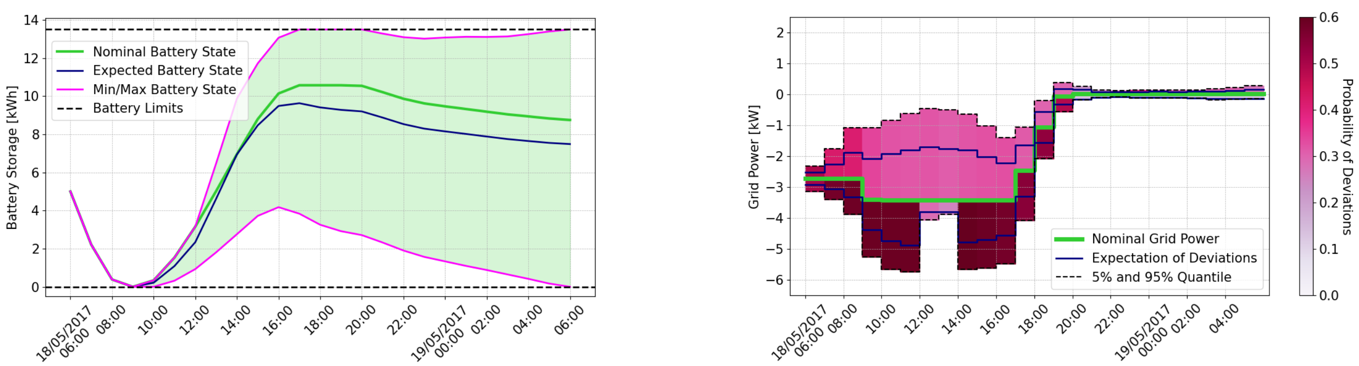


(e) Probabilistic BESS Schedule (f) Probabilistic Dispatch Schedule

Fig. 8: Case 3 - Reducing grid uncertainties during a critical timeframe. Between 12:00 and 14:00, the BESS is actively used to minimize downward deviations from the nominal grid power.

*3) Case 3:* The objective weights for Case 3 portray a trade-off between maximizing self-sufficiency and minimizing downward grid uncertainties between 12:00 and 14:00. In Figure 8f, the probabilities of upward grid deviations fluctuate around 30%. The probabilities of downward deviations during the critical timeframe drop to 25%, and the 5% quantiles are comparably close to the nominal grid power. However, the nominal battery state cannot reach its maximum limit, as some space is reserved for potential low prosumption realization, essentially providing flexibility for that critical timeframe.

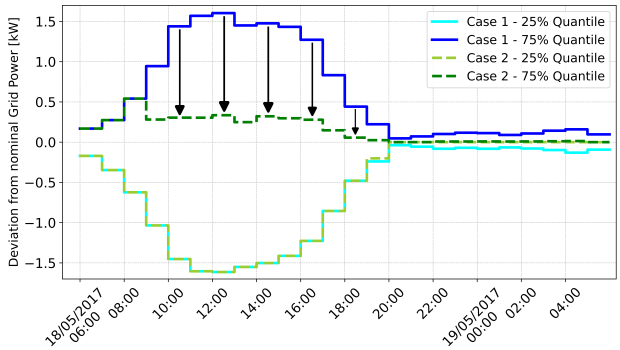


Fig. 9: Difference of selected grid power quantiles to the nominal grid power for Cases 1 and 2. The closer the quantiles to zero, the better. The grid uncertainty can be asymmetrically reduced by modeling both grid exchange and BESS probabilistically.

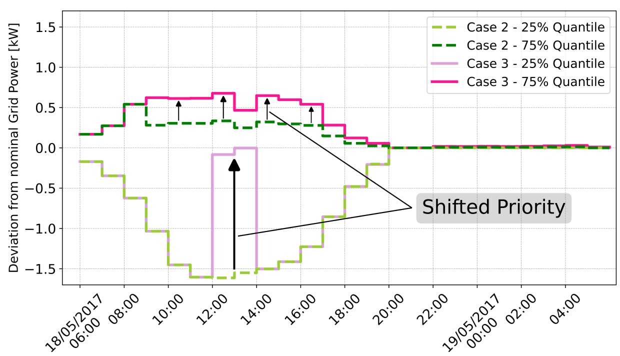


Fig. 10: Difference of selected grid power quantiles to the nominal grid power for Cases 2 and 3. The closer the quantiles to zero, the better. The model enables shifting the centered 50% prediction interval according to the user's needs.

### *C. Discussion*

Before we discuss the results, we want to clarify that our main contribution is manifested by obtaining both precisely quantified probabilistic BESS state and grid exchange schedules in Figures 7 and 8. With that, we are able to model both residential and grid desires, create a framework with a unifying perspective, and close the research gap described above. Nevertheless, it makes sense to discuss the experimental results in more detail, highlighting further key insights of the proposed model. First, we compare cases 1 and 2. Afterward, we compare cases 2 and 3 with each other.

*1) Comparison between Case 1 and Case 2:* In both cases, the nominal grid powers (and consequently also the nominal battery states) align. This indicates that both cases commit to the same nominal grid power schedule, which translates to a similar level of self-sufficiency. Downward deviations from the nominal grid power remain similar, with probabilities of around 60% for most of the day.

However, in Case 2, the probabilities of upward grid deviations drop to 25%, as compared to 40% in Case 1, as indicated by the shading in Figures 6b and 7d. This implies that with 15% probability, neither downward nor upward deviations occur. This is a key advantage of the proposed model. By incorporating a mixed random variable to model grid power uncertainties, the occurrence of discrete events with non-zero probability are enabled, i.e., with 15% probability can the nominal grid power be adhered to for Case 2. This becomes evident when comparing the theoretical grid power PDF in Figure 3c with the probabilistic DiSs. Here, the discrete green peak of Figure 3c corresponds directly to the green nominal grid power of Figures 6b and 7d. The only difference is that the discrete peak of Case 1 equals zero since all uncertainties are shifted towards the grid. For Case 2, the nonzero peak represents the cases where the BESS accounts for the full compensation of differences between expected and actual prosumption. Since both nominal grid powers align, this is achieved without having to make any compromises regarding the obtained level of residential self-sufficiency. As a result, an additional degree of freedom in residential BESS scheduling is identified: The tradeoff lies between reducing grid uncertainties and managing an unknown BESS state at the end of the schedule—a property further discussed in Section IV-D.

Furthermore, the narrower centered 50%-prediction interval in Figure 9 illustrates the advantages of modeling both grid and BESS probabilistically. Overall, this comparison demonstrates the model's ability to quantify and reduce grid uncertainties by exploiting the BESS's capacity, thereby enabling flexibility provision without neglecting residential objectives.

*2) Comparison between Case 2 and Case 3:* Case 3 extends the strategy used in Case 2 by providing flexibility during a critical period. This results in a tradeoff, as the nominal grid power in Case 3 reaches a lower plateau (-3.5 kW) than in Case 2 (-3 kW), reducing the household's self-sufficiency.

In both cases, the BESS is fully utilized to reduce grid uncertainties, i.e., the minimum and maximum battery states reach the battery limits. The key difference lies in when and how uncertainties are compensated. The areas above and below the nominal battery state serve as resources for reducing downward and upward grid uncertainties, respectively. Prioritizing downward uncertainty compensation lowers the nominal battery state, reducing its ability to handle upward uncertainties, as seen in Figure 10. There, the 25%-quantile of Case 3 is closer to zero than in Case 2, shifting the 75%-quantile further away. By adjusting the cost function weights $c_3$ and $c_4$, users can fine-tune prediction interval widths to align with their objectives, as illustrated by Case 3.

Ultimately, operators and residents must agree on the value of the investigated flexibility provision. This is particularly relevant in scenarios like Case 3, where the residential level of self-sufficiency is actively influenced by high weights $c_3$ or $c_4$. The specifics of financial compensation for flexibility provision, however, are beyond the scope of this paper and are only briefly discussed as part of the limitations.

### D. Limitations

The presented approach in its current form is purely designed for day-ahead planning, focusing on quantifying and distributing uncertainties rather than real-time operation. As a result, its performance is highly dependent on the quality of the probabilistic forecasts and does not capture operational costs. Moreover, our framework includes services that currently lack established financial counterparts, i.e., the transfer of historical prosumption data for model training and forecast creation, the day-ahead commitment of the BESS schedule, and the communication of the schedule to the grid operator. We aim to combine the residents' and grids' perspectives and integrate the BESS such that the overall system's added value can be maximized. This dual focus on residential and grid perspectives distinguishes our work from traditional cost-minimization approaches and makes direct cost comparisons and, thus, comparisons to other approaches difficult for the time being.

Another limitation of the model is the absence of a closed-form PDF to describe the probabilistic battery state, as discussed in Section II-E. While it is not possible to derive a function that fully captures the energy state due to the complexity of summing dependent random variables, key features of the distribution can still be derived, i.e., the minimum, maximum, nominal, and expected battery state. These states provide valuable insight, even though a full analytical representation of the PDF remains unavailable for the moment.

Furthermore, it can be noted that the minimum and maximum battery states typically reach the battery limits by the end of the optimization horizon. While grid uncertainties are penalized, uncertainties within the BESS are not, encouraging full use of the BESS's capacity. However, this does not guarantee a good starting point for upcoming scheduling tasks, especially if the prosumption is systematically over- or underestimated. Nevertheless, due to the characteristics of the presented model, the expected battery state at the end of the horizon will always be somewhere reasonable around half of the BESS's maximum capacity. If this outcome is still undesirable, it can be mitigated by adjusting the BESS constraints or introducing penalty terms to limit BESS exploitation.

Finally, it is important to recognize that forecasting prosumption essentially involves predicting human behavior. It is, therefore, a highly individual task, and forecasting templates, as they are investigated for automating wind and PV forecasting [43], are assumed to not be easily applicable to the presented methodology. Moreover, when looking at the probabilistic DiSs, it is important to note that exceptions outside of the 95% quantile can occur. Nevertheless, if those exceptions accumulate, good forecasting models should be able to catch up and adapt.

## V. Conclusion

We develop a stochastic continuous nonlinear optimization framework for residential day-ahead Battery Energy Storage System (BESS) scheduling. What distinguishes this work from others is the asymmetric allocation of quantified prosumption uncertainties between a residential BESS and the power grid. This is achieved by introducing mixed random variables to model both BESS and grid power uncertainties. With that, we place great emphasis not only on the BESS operation but also on the power exchange with the grid. The model is implemented and tested across several cases, demonstrating that residential BESS scheduling can effectively reduce grid uncertainties without compromising residential self-sufficiency. Moreover, during critical time periods, the BESS can be used proactively to mitigate grid uncertainties, contributing to a more resilient power grid. In summary, the proposed model empowers prosumers to actively support the power grid by managing uncertainties and offering flexibility. This presents a potential step towards a better integration of residential BESSs as valuable assets in modern power grids.

Future work will focus on extending the model to intraday scheduling and operation. Additionally, the model's performance in real-world research environments and the interaction between multiple buildings using this approach will be explored to assess its broader impact on the power grid.

## Acknowledgments

The authors thank the Helmholtz Association for the support under the "Energy System Design" program and the German Research Foundation as part of the Research Training Group 2153 "Energy Status Data: Informatics Methods for its Collection, Analysis and Exploitation".

## Declaration

For this work, the authors used ChatGPT during the writing process to improve clarity and fluency. After the usage, the authors reviewed and edited the content as needed and take full responsibility for the content of the published article.

## References

[1] K. Girigoudar, A. M. Hou, L. A. Roald, Chance-Constrained AC Optimal Power Flow for Unbalanced Distribution Grids, in: Proceedings of the 11th Bulk Power Systems Dynamics and Control Symposium (IREP), 2022. doi:10.48550/arXiv.2207.09520.

[2] K. V. Konneh, O. B. Adewuyi, M. E. Lotfy, Y. Sun, T. Senjyu, Application strategies of model predictive control for the design and operations of renewable energy-based microgrid: a survey, Electronics 11 (4) (2022) 554. doi:10.3390/electronics11040554.

[3] F. Sossan, E. Namor, R. Cherkaoui, M. Paolone, Achieving the dispatchability of distribution feeders through prosumers data driven forecasting and model predictive control of electrochemical storage, IEEE Trans. Sustain. Energy 7 (4) (2016) 1762–1777. doi:10.1109/TSTE.2016.2600103.

[4] S. Bahramara, Robust optimization of the flexibility-constrained energy management problem for a smart home with rooftop photovoltaic and an energy storage, J. Energy Storage 36 (2021) 102358. doi:10.1016/j.est.2021.102358.

[5] H. Haider, Y. Jun, G. I. Rashed, F. Peixiao, S. Kamel, Y. Li, A robust optimization model for microgrid considering hybrid renewable energy sources under uncertainties, Environ. Sci. Pollut. Res. Int. 30 (34) (2023) 82470–82484. doi:10.1007/s11356-023-27913-2.

[6] Y. Cao, L. Huang, Y. Li, K. Jermsittiparsert, H. Ahmadi-Nezamabad, S. Nojavan, Optimal scheduling of electric vehicles aggregator under market price uncertainty using robust optimization technique, Int. J. Electr. Power Energy Syst. 117 (2020) 105628. doi:10.1016/j.ijepes.2019.105628.

[7] M. R. Ebrahimi, N. Amjady, Adaptive robust optimization framework for day-ahead microgrid scheduling, Int. J. Electr. Power Energy Syst. 107 (2019) 213–223. doi:10.1016/j.ijepes.2018.11.029.

[8] R. Xie, Distributionally Robust Optimization and its Applications in Power System Energy Storage Sizing, Springer Nature, 2024.

[9] M. Rezaeimozafar, M. Duffy, R. F. Monaghan, E. Barrett, Residential pv-battery scheduling with stochastic optimization and neural network-driven scenario generation, Energy Rep. 12 (2024) 418–429. doi:10.1016/j.egyr.2024.06.017.

[10] Z. Wang, P. Jochem, W. Fichtner, A scenario-based stochastic optimization model for charging scheduling of electric vehicles under uncertainties of vehicle availability and charging demand, J. Clean. Prod. 254 (2020) 119886. doi:10.1016/j.jclepro.2019.119886.

[11] A. Tavakoli, A. Karimi, Development of Monte-Carlo-based stochastic scenarios to improve uncertainty modelling for optimal energy management of a renewable energy hub, IET Renew. Power Gener. 17 (5) (2023) 1139–1164. doi:10.1049/rpg2.12671.

[12] R. R. Appino, J. Á. G. Ordiano, R. Mikut, T. Faulwasser, V. Hagenmeyer, On the use of probabilistic forecasts in scheduling of renewable energy sources coupled to storages, Appl. Energy 210 (2018) 1207–1218. doi:10.1016/j.apenergy.2017.08.133.

[13] D. Werling, B. Heidrich, H. K. Çakmak, V. Hagenmeyer, Towards line-restricted dispatchable feeders using probabilistic forecasts for PV-dominated low-voltage distribution grids, in: Proceedings of the Thirteenth ACM International Conference on Future Energy Systems, 2022, pp. 395–400. doi:10.1145/3538637.3538868.

[14] B. Singh, B. Knueven, Lagrangian relaxation based heuristics for a chance-constrained optimization model of a hybrid solar-battery storage system, J. Glob. Optim. 80 (4) (2021) 965–989. doi:10.1007/s10898-021-01041-y.

[15] H. Su, Y. Zhou, D. Feng, H. Li, M. Numan, Optimal energy management of residential battery storage under uncertainty, Int. Trans. Electr. Energy Syst. 31 (2) (2021). doi:10.1002/2050-7038.12713.

[16] P. Scarabaggio, S. Grammatico, R. Carli, M. Dotoli, Distributed demand side management with stochastic wind power forecasting, IEEE Trans. Control Syst. Technol. 30 (1) (2021) 97–112. doi:10.1109/TCST.2021.3056751.

[17] X. Shi, Y. Xu, Q. Guo, H. Sun, X. Zhang, Day-Ahead Distributionally Robust Optimization-Based Scheduling for Distribution Systems with Electric Vehicles, IEEE Trans. Smart Grid 14 (4) (2022) 2837–2850. doi:10.1109/TSG.2022.3223332.

[18] S. S. Parvar, H. Nazaripouya, Optimal operation of battery energy storage under uncertainty using data-driven distributionally robust optimization, Electr. Power Syst. Res. 211 (2022) 108180. doi:10.1016/j.epsr.2022.108180.

[19] X. Xu, W. Hu, D. Cao, Q. Huang, Z. Liu, W. Liu, Z. Chen, F. Blaabjerg, Scheduling of wind-battery hybrid system in the electricity market using distributionally robust optimization, Renew. Energy 156 (2020) 47–56. doi:10.1016/j.renene.2020.04.057.

[20] H. Su, D. Feng, Y. Zhao, Y. Zhou, Q. Zhou, C. Fang, U. Rahman, Optimization of customer-side battery storage for multiple service provision: Arbitrage, peak shaving, and regulation, IEEE Trans. Ind. Appl. 58 (2) (2022) 2559–2573. doi:10.1109/TIA.2022.3145330.

[21] S. Sharda, M. Singh, K. Sharma, Demand side management through load shifting in IoT based HEMS: Overview, challenges and opportunities, Sustain. Cities Soc. 65 (2021) 102517. doi:10.1016/j.scs.2020.102517.

[22] A. Ciocia, A. Amato, P. Di Leo, S. Fichera, G. Malgaroli, F. Spertino, S. Tzanova, Self-consumption and self-sufficiency in photovoltaic systems: Effect of grid limitation and storage installation, Energies 14 (6) (2021) 1591. doi:10.3390/en14061591.

[23] N. Mlilo, J. Brown, T. Ahfock, Impact of intermittent renewable energy generation penetration on the power system networks–a review, Technol. Econ. Smart Grids Sustain. Energy 6 (1) (2021) 25. doi:10.1007/s40866-021-00123-w.

[24] B. Singh, Chance-constrained programming: joint and individual constraints, in: Encycl. Optim., Springer, 2023, pp. 1–5. doi:10.1007/978-3-030-54621-2_785-1.

[25] S. Beichter, M. Beichter, D. Werling, J. Galenzowski, V. Weise, C. Hildenbrand, F. Wiegel, R. Mikut, S. Waczowicz, V. Hagenmeyer, Towards a Real-World Dispatchable Feeder, in: 2023 8th IEEE Workshop on the Electronic Grid (eGRID), IEEE, 2023, pp. 1–6. doi:10.1109/eGrid58358.2023.10380834.

[26] P. M. Shankar, Probability, Random Variables, and Data Analytics with Engineering Applications, Springer, 2021.

[27] A. Papoulis, S. U. Pillai, Probability, random variables, and stochastic processes, McGraw-Hill Europe: New York, USA, 2002.

[28] C. Weld, L. Leemis, Modeling mixed type random variables, in: 2017 Winter Simulation Conference, IEEE, 2017, pp. 1595–1606. doi:10.1109/WSC.2017.8247900.

[29] W. Owen, T. DeRouen, Estimation of the mean for lognormal data containing zeroes and left-censored values, with applications to the measurement of worker exposure to air contaminants, Biometrics (1980). doi:10.2307/2556125.

[30] C. Li, V. P. Singh, A. K. Mishra, A bivariate mixed distribution with a heavy-tailed component and its application to single-site daily rainfall simulation, Water Resour. Res. 49 (2) (2013) 767–789. doi:10.1002/wrcr.20063.

[31] A. Groß, C. Wittwer, M. Diehl, Stochastic model predictive control of photovoltaic battery systems using a probabilistic forecast model, Eur. J. Control 56 (2020) 254–264. doi:10.1016/j.ejcon.2020.02.004.

[32] F. Pacaud, P. Carpentier, J.-P. Chancelier, M. De Lara, Optimization of a domestic microgrid equipped with solar panel and battery: Model predictive control and stochastic dual dynamic programming approaches, Energy Syst. 15 (1) (2022) 115–139. doi:10.1007/s12667-022-00522-7.

[33] P. F. Austnes, C. García-Pareja, F. Nobile, M. Paolone, Probabilistic Load Forecasting of Distribution Power Systems based on Empirical Copulas, Preprint Sustain. Energy Grids Netw. (2023). doi:10.48550/arXiv.2310.03657.

[34] H. Brass, K. Petras, Quadrature theory: the theory of numerical integration on a compact interval, American Math. Soc., 2011.

[35] M. L. Bynum, G. A. Hackebeil, W. E. Hart, C. D. Laird, B. L. Nicholson, J. D. Siirola, J.-P. Watson, D. L. Woodruff, Pyomo–optimization modeling in Python, 3rd Edition, Vol. 67, Springer Science & Business Media, 2021.

[36] A. Wächter, L. T. Biegler, On the implementation of an interior-point filter line-search algorithm for large-scale nonlinear programming, Math. Program. 106 (2006) 25–57. doi:10.1007/s10107-004-0559-y.

[37] J. Pinter, Day-Ahead Battery Scheduling based on Mixed Random Variables (Mar. 2025).
URL https://github.com/JaMoPinter/Day-Ahead-Battery-Scheduling

[38] Open Power System Data, Data Package Household Data, https://data.open-power-system-data.org/household_data/2020-04-15, accessed: September 20, 2024 (2020).

[39] K. G. Olivares, C. Challú, F. Garza, M. M. Canseco, A. Dubrawski, NeuralForecast: User friendly state-of-the-art neural forecasting models., PyCon Salt Lake City, Utah, US 2022 (2022).
URL https://github.com/Nixtla/neuralforecast

[40] Y. Nie, N. H. Nguyen, P. Sinthong, J. Kalagnanam, A time series is worth 64 words: Long-term forecasting with transformers, in: International Conference on Learning Representations, 2023. doi:10.48550/arXiv.2211.14730.

[41] H. K. Çakmak, V. Hagenmeyer, Using open data for modeling and simulation of the all electrical society in eASiMOV, in: Open Source Modelling and Simulation of Energy Systems (OSMSES), IEEE, 2022, pp. 1–6. doi:10.1109/OSMSES54027.2022.9769145.

[42] Tesla, How Powerwalls work, https://www.tesla.com/support/energy/powerwall/learn/how-powerwall-works, accessed: September 19, 2024.

[43] S. Meisenbacher, B. Heidrich, T. Martin, R. Mikut, V. Hagenmeyer, AutoPV: Automated photovoltaic forecasts with limited information using an ensemble of pre-trained models, in: Proceedings of the 14th ACM International Conference on Future Energy Systems, 2023, pp. 386–414. doi:10.1145/3575813.3597348.

**Declaration of interests**

☒ The authors declare that they have no known competing financial interests or personal relationships that could have appeared to influence the work reported in this paper.

☐ The authors declare the following financial interests/personal relationships which may be considered as potential competing interests: